A Homogeneous Fluorescence Resonance Energy Transfer System for Monitoring the Activation of a Protein Switch in Real Time

Anke Bill,[†] Heike Blockus,[†] Dagmar Stumpfe,[‡] Jürgen Bajorath,[‡] Anton Schmitz,[†] and Michael Famulok*,[†]

[†]LIMES Institute, Chemical Biology and Medicinal Chemistry Unit, c/o Kekulé Institute of Organic Chemistry and Biochemistry, University of Bonn, Gerhard-Domagk-Strasse 1, 53121 Bonn, Germany

[‡]LIMES Institute, Chemical Biology and Medicinal Chemistry Unit, Department of Life Science Informatics, B-IT, University of Bonn, Dahlmannstrasse 2, 53113 Bonn, Germany

Ⓢ *Supporting Information*

ABSTRACT: A homogeneous fluorescence resonance energy transfer (FRET) system for the real-time monitoring of exchange factor-catalyzed activation of a ras-like small GTPase is described. The underlying design is based on supramolecular template effects exerted by protein−protein interactions between the GTPase adenosine diphosphate ribosylation factor (ARF) and its effector protein GGA3. The GTPase is activated when bound to guanosine triphosphate (GTP) and switched off in its guanosine diphosphate (GDP)-bound state. Both states are accompanied by severe conformational changes that are recognized by GGA3, which only binds the GTPase "on" state. GDP-to-GTP exchange, i.e., GTPase activation, is catalyzed by the guanine nucleotide exchange factor cytohesin-2. When GGA3 and the GTPase ARF1 are labeled with thoroughly selected FRET probes, with simultaneous recording of the fluorescence of an internal tryptophan residue in ARF1, the conformational changes during the activation of the GTPase can be monitored in real time. We applied the FRET system to a multiplex format that allows the simultaneous identification and distinction of small-molecule inhibitors that interfere with the cytohesin-catalyzed ARF1 activation and/or with the interaction between activated ARF1-GTP and GGA3. By screening a library of potential cytohesin inhibitors, predicted by in silico modeling, we identified new inhibitors for the cytohesin-catalyzed GDP/GTP exchange on ARF1 and verified their increased potency in a cell proliferation assay.
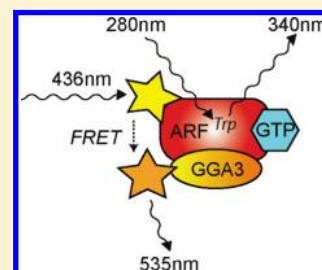
■ INTRODUCTION

Adenosine diphosphate ribosylation factors (ARFs), small guanine nucleotide-binding proteins of the Ras superfamily, control essential cellular functions including cytoskeletal dynamics, cell migration, and vesicular trafficking.[1] Like all small GTPases, ARFs are molecular switches that cycle between two conformations: the active guanosine triphosphate (GTP)-bound conformation and the inactive guanosine diphosphate (GDP)-bound state. ARF activity is tightly controlled by regulatory proteins: GTPase-activating proteins (GAPs) inactivate the ARFs by stimulating their intrinsic GTP hydrolase activity, and guanine nucleotide exchange factors (GEFs) activate the ARFs by facilitating the dissociation of GDP and the binding of GTP.[2]

The ARF GEFs of the cytohesin family consist of four highly homologous members: cytohesin-1, cytohesin-2 (ARNO), cytohesin-3, and cytohesin-4. Cytohesins belong to the class of small ARF GEFs. They share a conserved domain structure, namely the amino-terminal coiled-coil domain, which is used for interaction with cellular binding partners, the central Sec7 domain, which harbors the GEF function, and the carboxy-terminal pleckstrin homology (PH) domain, which can bind to inositol phospholipids and therefore regulate the protein's membrane association.[3] In contrast to large ARF GEFs that primarily regulate Golgi-localized ARFs, cytohesins control ARFs in particular at the plasma membrane and in the endosomal pathway.[1,3] Furthermore, cytohesins have been shown to be involved in signal transduction of receptor tyrosine kinases, like the ErbB or insulin receptors.[4−7]

Upon activation of ARF, significant conformational changes occur that are accompanied by a change in the intrinsic tryptophan fluorescence of the protein.[8] Therefore, the most widely applied ARF activation assay measures tryptophan excitation and emission at 280 and 340 nm, respectively. In most cases, a truncated version of ARF1 (NΔ17ARF1) is used, which renders the assay independent of lipid membranes and increases the solubility of ARF1.[8,9] An alternative approach to measure the GEF-catalyzed activation of NΔ17ARF1 is to use GDP or GTP analogues labeled with an environmentally sensitive fluorescent group, like *N*-methylanthraniloyl (or mant).[10,11] The fluorescence of mant-GDP/GTP exhibits both an increased fluorescence quantum yield and a blue-shift of 10−20 nm in its fluorescence emission maximum upon protein binding. Mant-guanine nucleotides can be excited at a wavelength of 360 nm and show protein-binding-dependent emission at 440 nm, remote from the wavelength region where proteins or most small molecules absorb. By using

mant-nucleotides, activation of NΔ17ARF1 can be followed kinetically in three ways. First, one can simply monitor binding of mant-GTP to NΔ17ARF1 by measuring the fluorescence of mant-GTP at ex360/em440 nm. As a variant, the displacement of mant-GDP by GTP on mant-GDP-preloaded NΔ17ARF1 can also be measured. Furthermore, it is possible to use fluorescence resonance energy transfer (FRET) between tryptophan and mant-nucleotide to follow the exchange reaction (ex280/em440 nm). Here the tryptophan residue is excited and acts as a donor to induce the fluorescence of the acceptor mant group. Although the mant fluorescent group is small and in general does not disturb the binding of small molecules, possible interference has to be taken into account.

A different, fluorescence-independent approach to measure GDP/GTP exchange on NΔ17ARF1 makes use of radioactively labeled nucleotides.[12] For this purpose, the exchange reaction is conducted in the presence of radioactively labeled GTP. GTP loading on NΔ17ARF1 is measured after removal of unbound radioactivity, e.g., by filter binding. However, because of the nonhomogenous nature of the assay, determination of kinetic parameters is difficult.

The latter group of assays is based on the specific interactions of activated ARF proteins with their effector proteins. By specifically binding to ARF-GTP, these proteins are recruited to cellular membranes where they initiate, e.g., the formation of transport vesicles.[13] The GAT domain of GGAs (Golgi-localized, gamma ear-containing, ARF-binding proteins) specifically interact with ARF-GTP and can be used as a tool to quantify the amount of ARF-GTP in vitro and in vivo.[14,15] For this purpose, a GST-tagged GGA-GAT domain is added to an exchange reaction or cell lysate. After precipitation of GGA-GAT, the amount of bound ARF-GTP is determined by SDS-PAGE and Western blotting. The strength of this pull-down technique is that it gives information about the amount of activated ARF in complex samples like cell lysates. None of these assays allows the simultaneous real-time measurement of both the activation of ARF and its activation-dependent interaction with an effector protein, which would provide valuable information not only about the bioactivity of ARF and its effectors but also about how a given small molecule might inhibit ARF.

Here we describe a new, homogeneous FRET system that allows for the monitoring of cytohesin-catalyzed GDP/GTP exchange on NΔ17ARF1. The principal design relies on supramolecular template effects of protein–protein interactions that depend on the activation status of one partner and the labeling of these partners with carefully selected FRET probes. Only when activated by a bound small-molecule ligand, guanosine triphosphate GTP, do the corresponding structural changes enable the association of the other partner. When the activation is catalytically triggered by the guanine nucleotide exchange factor ARNO (cytohesin-2), the simultaneous monitoring of both the guanine nucleotide exchange factor-catalyzed exchange of GDP for GTP that leads to the activation of the Ras-like small GTPase ARF1 and the consequence of this activation, namely the interaction of the activated ARF with one of its specific effector proteins, GGA3, becomes possible. The system also allows the simultaneous identification and distinction of small-molecule inhibitors that interfere with the cytohesin-catalyzed NΔ17ARF1 activation and/or with the interaction between NΔ17ARF1-GTP and its effector protein GGA3. By applying this FRET system, we identified new inhibitors for the cytohesin-catalyzed GDP/GTP exchange on NΔ17ARF1.
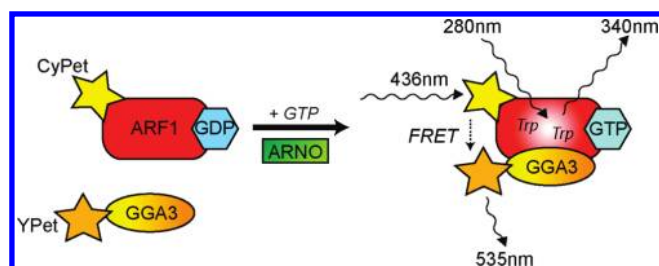

Figure 1. FRET system for the cytohesin-catalyzed GDP/GTP exchange on NΔ17ARF1: principle of the assay. GDP-preloaded NΔ17ARF1-CyPet is incubated with ARNO-Sec7 and YPet-GGA3. The exchange reaction is started by addition of GTP. The conformational change in NΔ17ARF1-CyPet caused by GDP/GTP exchange is detected by measuring tryptophan fluorescence (ex280/em340 nm). Simultaneously, the amount of GTP-loaded NΔ17ARF1-CyPet is monitored by FRET (ex436/em535 nm) resulting from the interaction of NΔ17ARF1-CyPet-GTP with YPet-GGA3.

■ RESULTS

FRET System for Cytohesin-Catalyzed GDP/GTP Exchange on NΔ17ARF1. By monitoring the tryptophan fluorescence of NΔ17ARF1-CyPet simultaneously with the FRET between NΔ17ARF1-CyPet and YPet-GGA3, our real-time, homogeneous FRET system measures two results of GTP binding to ARF: the conformational change of ARF itself and the interaction with the effector GGA3. Based on this dual detection, it is possible to identify both kinds of inhibitors, those that interfere with the cytohesin-catalyzed nucleotide exchange on ARF1 and inhibitors that block binding of GTP-loaded ARF1 to its effector protein.

Figure 1 displays the principles of the FRET system. NΔ17ARF1 was C-terminally tagged with the fluorescent protein CyPet. NΔ17ARF1-CyPet is nonenzymatically preloaded with GDP and subsequently incubated with the Sec7 domain of ARNO. To monitor binding of NΔ17ARF1-CyPet-GTP to its effector protein GGA3, GGA3-GAT domain with its N-terminus fused to the fluorescent protein YPet is added. After starting the exchange reaction by addition of GTP, NΔ17ARF1-CyPet activation is detected by measuring tryptophan fluorescence at ex280/em340 nm. Simultaneously, binding of NΔ17ARF1-CyPet-GTP to YPet-GGA3 is analyzed in real time by FRET between the CyPet moiety of NΔ17ARF-CyPet and the YPet moiety of YPet-GGA3 at ex436/em535 nm. CyPet is excited at 436 nm and acts as a donor to induce fluorescence of YPet. CyPet and YPet are FRET-optimized variants of the fluorescent proteins CFP and YFP, respectively, and have been recently used to monitor ARF6 activation in living cells.[16,17] Since fluorescence energy transfer critically depends on the proximity of the two fluorophores involved, binding of GTP-loaded NΔ17ARF-CyPet to YPet-GGA3 leads to an increase in FRET between CyPet and YPet, and therefore to enhanced emission of YPet at 535 nm.

Activation of ARF1-CyPet Can Be Monitored in Real Time by Simultaneous Detection of Tryptophan Fluorescence and FRET in the Presence of YPet-GGA3. To exclude that YPet-GGA3 disturbs the ARNO-Sec7-catalyzed GDP/GTP exchange on NΔ17ARF-CyPet, we added increasing amounts of YPet-GGA3 (0.2−1.0 μM) to an exchange reaction (0.7 μM NΔ17ARF-CyPet, 15 nM ARNO-Sec7). All measurements were performed in PBS, pH 7.4, 3.0 mM MgCl$_2$ at 37 °C in black 96-well plates, in a total volume of 200 μL.
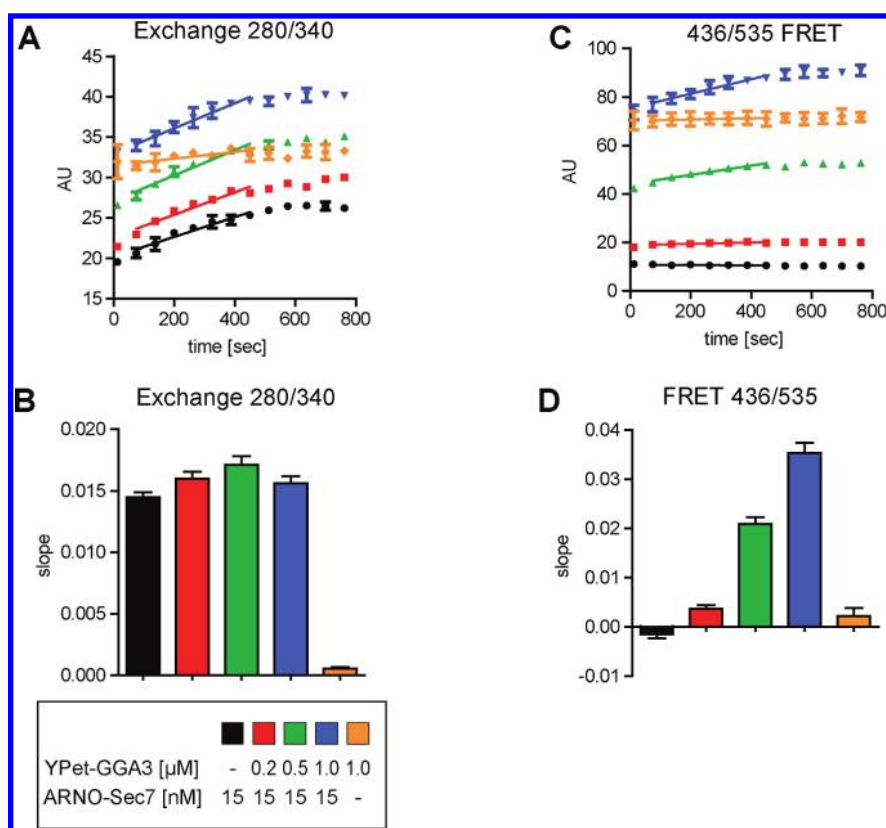
Figure 2. Simultaneous measurement of tryptophan fluorescence and FRET in a homogeneous assay format. (A,C) Tryptophan fluorescence ex280/ em340 nm (A) or FRET ex436/em535 nm (C) of NΔ17ARF1-CyPet in the presence (black, red, green, blue) or absence (orange) of ARNO-Sec7 and different concentrations of YPet-GGA3 (red, green, blue). The slope of the reaction was calculated by fitting the linear part of the increase in tryptophan fluorescence or FRET by linear regression (shown as a line). (B,D) Calculated slope for the initial increase in tryptophan fluorescence (B) or FRET signal (D). Data represent the means ± SEM of duplicates of one representative measurement (out of three independent measurements). For fluorescence measurements of YPet and CyPet, please refer to Supporting Information Figure S1.

Figure 2 shows the signals obtained at 280/340 nm (Figure 2A, tryptophan fluorescence = exchange) and 436/535 nm (Figure 2C, FRET = interaction between NΔ17ARF-CyPet-GTP and YPet-GGA3) as well as the calculated slopes for the initial, linear phase of the reaction (Figure 2B,D). As expected, GDP/GTP exchange on NΔ17ARF-CyPet critically depends on the presence of ARNO-Sec7 (Figure 2A,B; compare black and orange bars). Although increasing amounts of YPet-GGA3 raised the fluorescence signal at the starting point due to higher absolute protein concentrations, they did not influence the slope of the reaction (red, green, blue). Thus, YPet-GGA3 does not interfere with the Sec7-catalyzed exchange reaction. No FRET signal could be detected in the absence of YPet-GGA3 (black, Figure 2C,D). As expected, increasing amounts of YPet-GGA3 enhanced the FRET signal (red, green, blue) due to increased complex formation between Δ17ARF-CyPet-GTP and YPet-GGA3. In agreement with the tryptophan fluorescence, only a weak FRET signal was detected in the absence of ARNO-Sec7, even at the highest concentration of YPet-GGA3 (orange). On the basis of these results, a concentration of 0.5 μM of YPet-GGA3 was selected for further experiments. Taken together, these data show that fusion of Δ17ARF1 with CyPet does not interfere with its Sec7-dependent activation and that the FRET signal obtained for the interaction of Δ17ARF-CyPet and YPet-GGA3 critically depends on the loading of Δ17ARF-CyPet with GTP.

To demonstrate that Δ17ARF-CyPet-GTP can be detected with the FRET-based exchange assay in a quantitative manner,

we conducted exchange assays in the presence of increasing concentrations of ARNO-Sec7 (3.5−30 nM) or Δ17ARF-CyPet (0.1−1.3 μM). As expected, the measured slopes for the tryptophan fluorescence (Figure 3A) directly depend on the concentration of ARNO-Sec7 and Δ17ARF-CyPet, reflecting increasing concentrations of Δ17ARF-CyPet-GTP. The slopes of the signals obtained for the FRET between Δ17ARF-CyPet-GTP and YPet-GGA3 (Figure 3B) directly mirrored the slopes of the tryptophan fluorescence, demonstrating the suitability of this assay to quantitatively monitor the GDP/GTP exchange on Δ17ARF1.

We next examined whether the FRET-based exchange assay is suited for detecting the chemical inhibition of cytohesins by the cytohesin antagonists SecinH3 and Secin16.[6,18] For this purpose we performed an exchange assay on Δ17ARF1-CyPet in the presence of SecinH3 (15 μM), Secin16 (2.5 μM), or solvent (1% DMSO). Figure 4 shows that inhibition of ARNO-Sec7 with SecinH3 or Secin16 is detected by a reduced slope in both the tryptophan fluorescence (Figure 4A) and the FRET signal (Figure 4B). Again, both detection methods revealed consistent results.

To test the suitability of the FRET-based GDP/GTP exchange assay on Δ17ARF1-CyPet for use as a screening assay, we determined the Z′ factor.[19] This factor reflects both the dynamic range of the signals (or the signal-noise-ratio) and the variation of the obtained signals. The Z′ factor is therefore a useful tool to
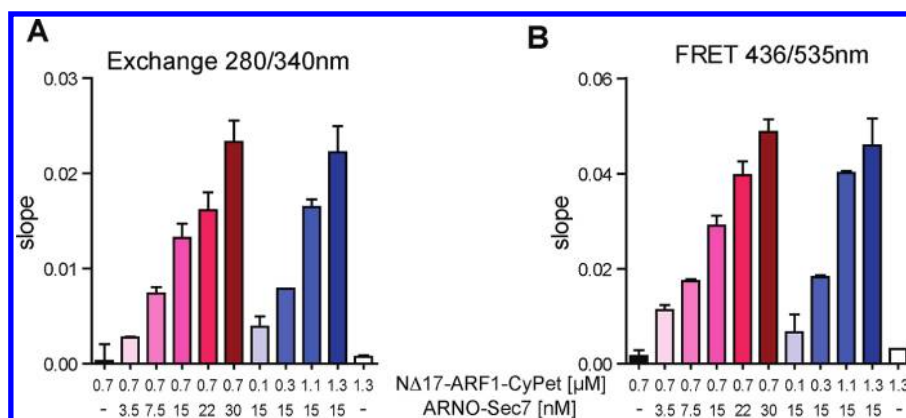
Figure 3. FRET-based determination of activated ARF. Calculated slope for the initial increase in tryptophan fluorescence (A) or FRET signal (B). Increasing concentrations of ARNO-Sec7 (0−30nM) were titrated to 0.7 μM NΔ17ARF1-CyPet (red bars), or the concentration of NΔ17ARF1-CyPet was varied in the presence of 15 nM ARNO-Sec7 (blue bars). All measurements were preformed in the presence of 0.5 μM YPet-GGA3. Data represent the means ± SEM of duplicates of one representative measurement (out of three independent measurements).
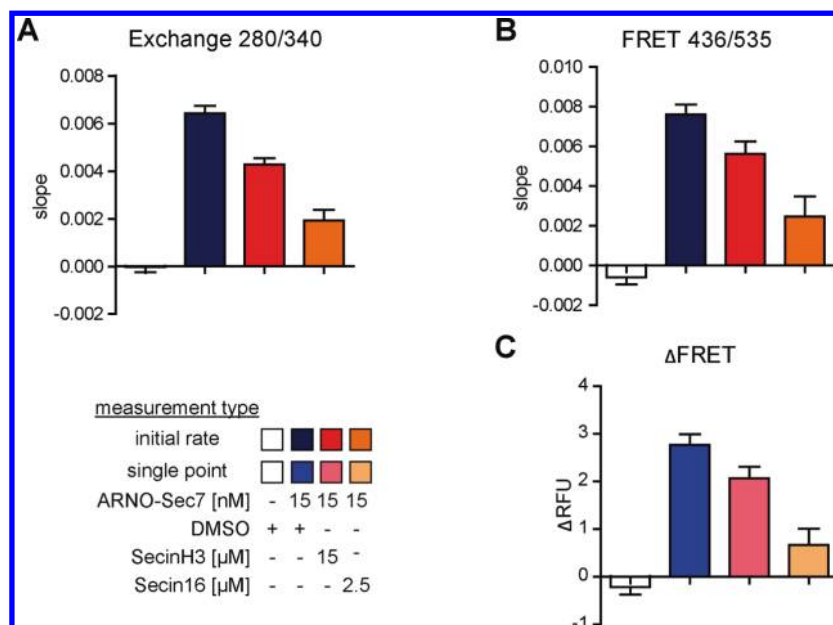

Figure 4. Suitability of the FRET and tryptophan fluorescence system to detect inhibitors of ARF activation. (A,B) Calculated slope for the initial increase in tryptophan fluorescence (A) or FRET signal (B) of NΔ17ARF1-CyPet (0.7 μM) in the presence of 15 μM SecinH3 (red), 2.5 μM Secin16 (orange), or solvent (0.4% DMSO, blue). All measurements were performed in the presence of 0.5 μM YPet-GGA3. (C) Simplified data analysis by calculating the difference in the FRET signal between the beginning and the end of the exchange reaction (ΔFRET). ΔFRET was calculated as the difference of the means of three single measurement values at the end (580−600 s) and the beginning (200−220 s) of the reaction. ΔFRET = MEAN$_{END}$(v$_{600s}$,v$_{590s}$,v$_{580s}$) − MEAN$_{START}$(v$_{220s}$,v$_{210s}$,v$_{200s}$). Data represent the means of five independent measurements.

describe the quality of an assay system. For the tryptophan fluorescence as well as for FRET-based detection of GDP/GTP exchange on Δ17ARF1-CyPet, we calculated a Z' factor of 0.6 out of six independent measurements, with the reactions in the presence or absence of ARNO-Sec7 used as a positive or negative control, respectively. This Z' value rates the FRET and tryptophan fluorescence detection system as being reliable and accurate, and even potentially suitable for screening.

In order to allow the testing of larger sets of compounds, we asked whether it might be possible to simplify data analysis. Therefore, we calculated the difference in the FRET signal (ΔFRET) between the beginning (∼200 s after GTP addition) and the end point (∼600 s) of the linear phase of the reaction

(Figure 4C). To minimize technically caused variations in single-point fluorescence measurements, we used the mean of three time points to calculate the difference in fluorescence signal (ΔFRET), i.e., ΔFRET = MEAN$_{END}$(v$_{600s}$,v$_{590s}$,v$_{580s}$) − MEAN$_{START}$(v$_{220s}$,v$_{210s}$,v$_{200s}$). In the presence of SecinH3 or Secin16, we observed a decrease in ΔFRET which closely mirrored the reduced initial slope determined as above (compare panels D and C of Figure 4). Again, we determined the Z' factor for this kind of analysis to rate its suitability for screening assays. Although the Z' factor of 0.5 was lower than the Z' factor calculated for the analysis of the initial slope of the exchange reaction, it still fit the requirements for a screening assay.
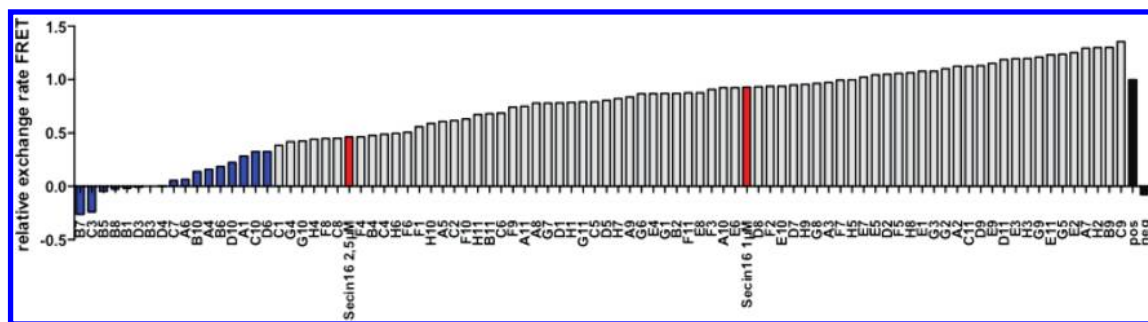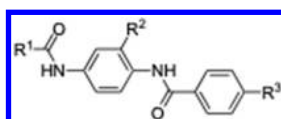
8375

dx.doi.org/10.1021/ja202513s |*J. Am. Chem. Soc.* 2011, 133, 8372–8379

Figure 5. Screening of 88 Secin16-analogues. GDP/GTP exchange on NΔ17ARF1-CyPet in the presence of the 88 Secin16 analogues (1.0 μM) or Secin16 (1.0 μM, 2.5 μM) as detected by FRET between NΔ17ARF1-CyPet and YPet-GGA3. Shown are the relative exchange rates, calculated as the slopes of the initial increase in FRET signal with the reaction in the presence of solvent only set to 1 (black). Seventeen hits were identified that inhibited the reaction more than 70% (blue bars).

Table 1. Structures of 17 Secin16 Analogues That Showed at Least 70% Inhibition of GDP/GTP Exchange on Δ17ARF1-CyPet at a Concentration of 1.0 μM

Screening of Secin16-Derived Chemotypes.

High-throughput screening currently plays a major role as a source of novel active molecules that serve as leads for drug development and as tools for biomedical research. As an alternative, virtual screening of chemical libraries formatted in silico can be applied to search for new chemotypes. Starting from SecinH3 analogues as virtual screening templates, we recently identified structurally distinct Sec7 inhibitors including Secin16.[18] Here we used Secin16 as a template and explored its chemical neighborhood using a fingerprint search. Publicly available compounds were ranked in the order of decreasing similarity to Secin16. From this ranking, different Secin16 analogues and structurally distinct molecules were selected, yielding a library of potential Sec7 inhibitors that contained 88 commercially available compounds.

These compounds were tested for their potential to inhibit the GDP/GTP exchange on Δ17ARF1-CyPet at a concentration of 1.0 μM using the dual-detection exchange assay. By analyzing the initial rate of FRET signal increase, we identified 17 compounds that showed at least 70% inhibition (Figure 5, blue bars; Secin16 red bars), which were classified as hits. The structures of these compounds are shown in Table 1.
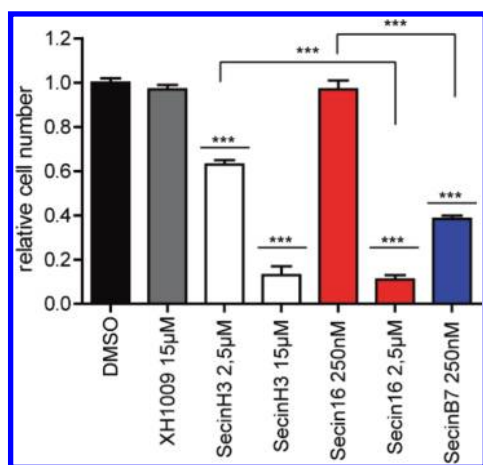
8376

dx.doi.org/10.1021/ja202513s |*J. Am. Chem. Soc.* 2011, 133, 8372–8379

Figure 6. Effect of Secin analogues on PC9 cell proliferation. SecinH3, Secin16, and SecinB7 but not the control compound XH1009 inhibit proliferation of PC9 cells. The diagram shows the relative cell number (MTT assay) after 72 h treatment with the indicated compounds or DMSO. The cell number in the solvent treated samples was set to 1. ***, $p > 0.001$, $n \geq 3$.

The simplified single-point evaluation of the FRET signal identified the same 17 hits, underlining the equivalence of both methods of analysis.

By analyzing the tryptophan fluorescence of Δ17ARF1-CyPet, 19 hits were found. These 19 compounds included all 17 hits identified in the FRET-based analyses. One compound, F6, showed an inhibition of 74% in tryptophan fluorescence and 51% (initial rate) or 60% (ΔFRET) inhibition in the FRET-based detection. H1 completely inhibited the increase in tryptophan fluorescence but was only moderately active in the FRET-based measurements. Re-evaluation of the data revealed the inhibition in the tryptophan fluorescence assay as a quenching artifact caused by strong absorption of H1 at 280 nm. The ability to easily identify H1 as a false-positive hit in the tryptophan fluorescence assay exemplifies an important advantage of our dual-detection exchange assay. In addition, 10 compounds showed strong autofluorescence at 280/340 nm and could hence only be evaluated in the FRET-based assay. Compound B7 showed the strongest inhibition in both assays and was re-evaluated at different concentrations to verify dose-dependency and to determine an IC$_{50}$ value. With an IC$_{50}$ of 0.44 ± 0.06 μM, B7 showed a nearly 10-fold or even 26-fold improved potency compared to Secin16 (3.74 ± 0.37 μM) or SecinH3 (11.40 ± 0.70 μM).

Effect of Secin Analogues on PC9 Cell Proliferation. Recently it was shown that cytohesins are involved in the regulation of PC9 cell proliferation.[4] We therefore performed a proliferation assay of PC9 cells in the presence of Secin analogues to verify the improved potency of SecinB7 in cells. As a negative control we used either DMSO or the compound XH1009, a derivative of the cytohesin inhibitor SecinH3 that does not act on cytohesins. We also tested SecinH3 and Secin16 to compare their effects directly with that of SecinB7. Figure 6 shows that SecinB7 significantly inhibited PC9 cell proliferation at 250 nM, a concentration at which neither SecinH3 nor Secin16 exhibits detectable activity, demonstrating its improved potency as compared with these first- and second-generation Secins.

■ DISCUSSION

Our study introduces a new measuring paradigm that allows simultaneous monitoring of both the GEF-catalyzed nucleotide exchange on a small GTPase and the result of the exchange, i.e., the interaction of the activated GTPase with one of its effector proteins, GGA3. The FRET system combines the advantages of rapid and highly sensitive real-time fluorescence measurements with the possibility to identify small-molecule inhibitors of the interaction between NΔ17ARF1-GTP and GGA3. Thus, it allows the simultaneous identification and distinction of small-molecule inhibitors that interfere with cytohesin-catalyzed NΔ17ARF1 activation and/or with the interaction between NΔ17ARF1-GTP and its effector protein GGA3.

Up-regulated activity of small GTPases is involved in various human diseases. This is not only true for the prototype oncogene ras. ARFs play an important role in the regulation of the proliferation and invasive capacity of cancer cells, making them attractive targets for cancer therapy.[20−23] Unfortunately, no specific, direct ARF inhibitor has been described. However, indirect inhibition of ARFs by targeting their specific GEFs has been proven very useful to elucidate the cellular functions of ARFs. The fungal metabolite brefeldin A (BFA) binds to the complex of GDP-bound, inactive ARF1 and the Sec7 domain of large GEFs, thereby inhibiting GDP/GTP exchange catalyzed by this subgroup of GEFs.[24] By a similar mechanism, the small molecule LM11 targets the complexes of ARF1-GDP with the large GEF BIG1 as well as with BFA-insensitive ARNO. Both molecules have been shown to inhibit ARF-regulated traffic at the Golgi apparatus in cells.[25] Recently, we have described the two cytohesin-specific inhibitors, SecinH3 and Secin16 (**Sec**7 **in**hibitors),[6,18,26,27] and various studies have proven their potential as indirect inhibitors of ARF1 and ARF6.[5,6,18,28−32] However, in order to elucidate the cellular role of a particular ARF or its corresponding ARF-GEF, monospecific ARF and ARF-GEF inhibitors are required. We showed in this study that the FRET system developed here can also serve as a new multiplex assay for the simultaneous identification of ARF and ARF-GEF inhibitors by applying it to a new set of Secin candidates, predicted by in silico modeling.

Since the presence of YPet-GGA3 did not affect GDP/GTP exchange on NΔ17ARF1-CyPet, it is possible to perform the FRET-based assay in a homogeneous format. Interaction between NΔ17ARF1-CyPet and YPet-GGA3 can be detected in real time, simultaneously with tryptophan fluorescence. These features enable the identification and discrimination of cytohesin inhibitors, ARF1 inhibitors, and inhibitors of the interaction between ARF1-GTP and its effector protein GGA3 in one single, homogeneous, real-time measurement.

By screening a set of 88 potential Sec7-domain inhibitors, predicted by virtual screening, we were able to identify 17 novel chemotypes that inhibited GDP/GTP exchange on ARF1 by more than 70% at a concentration of 1.0 μM in both tryptophan fluorescence and FRET measurements. The most potent molecule, termed SecinB7, showed an IC$_{50}$ < 500 nM, a nearly 10-fold improvement in potency compared to the template compound Secin16. This improved potency was verified in a cellular context by inhibiting cytohesin-dependent PC9 cell proliferation.

Eleven compounds showed a strong absorption and/or autofluorescence in the tryptophan fluorescence assay, making it impossible to analyze these compounds by this commonly used exchange assay. However, all 11 compounds could be

8377

dx.doi.org/10.1021/ja202513s | *J. Am. Chem. Soc.* 2011, 133, 8372–8379

investigated by the FRET-based exchange assay, and one compound was identified as a false positive. No compound showed an interference with the fluorescence measurement at the wavelength used for FRET, underlining the considerable advantage of using longer wavelengths for the screening of small molecules.

No compound was identified that inhibited the interaction between NΔ17ARF1-CyPet-GTP and YPet-GGA3 without disturbing the cytohesin-catalyzed exchange on NΔ17ARF1. The explanation lies in the limited structural variability of the 88 test compounds that were derived from the cytohesin inhibitor Secin16. Our results not only introduce a new, powerful FRET system for the identification of small-molecule inhibitors of cytohesin or ARF proteins. The same measuring principle also provides a means for the simultaneous monitoring of both the guanine nucleotide exchange factor-catalyzed exchange of GDP for GTP on NΔ17ARF1, leading to activation of this Ras-like small GTPase, and the consequence of this activation, i.e., the interaction of the activated ARF with one of its specific effector proteins, GGA3. The same principle should also be applicable to other combinations of GEF, GTPase, and effector proteins, and thus can serve as a useful modular tool for the rapid in vitro determination of these activities in various biological contexts.

■ METHODS

Constructs and Proteins. For the construction of the CyPet and YPet constructs, CyPET-Arf6 (Addgene plasmid 18840) and YPet-GGA3 (Addgene plasmid 18841) were used as templates.[16] NΔ17ARF1-CyPet (amino acids 18−181 of human ARF1 fused to the N-terminus of CyPet), YPet-GGA3 (YPet fused to amino acids 148−302 of human GGA3), and ARNO-Sec7 (amino acids 50−255) were subcloned into pET15 vectors (Novagen). All proteins were N-terminally 6xHis-tagged, expressed in *Escherichia coli*, and purified by Ni^{2+}-NTA chromatography (Ni-NTA agarose, Qiagen).

Exchange Assay. All measurements were performed in PBS pH 7.4, 3.0 mM $MgCl_2$ at 37 °C. NΔ17ARF1-CyPet (2.8 μM) was preincubated with GDP (80 μM) in the presence of EDTA (2.0 mM) for 15 min in PBS pH 7.4 at 37 °C. The bound GDP was stabilized by addition of $MgCl_2$ (final concentration 3.0 mM) and incubation for a further 5 min at 37 °C. If not otherwise indicated, 700 nM of GDP-loaded NΔ17ARF1-CyPet was mixed with 15 nM ARNO-Sec7 in the absence or presence of inhibitor or solvent (1% DMSO) in PBS pH 7.4, 3.0 mM $MgCl_2$, and after 5 min incubation at room temperature, 500 nM YPet-GGA3 was added (total volume 180 μL). The reaction was started by injection of 20 μL of GTP (50 μM). Fluorescence was detected approximately every 10 s, depending on sample number, for a total of 600 s. The tryptophan fluorescence was measured at excitation and emission wavelengths of 280 and 340 nm, respectively, whereas FRET was measured at 436 and 535 nm, respectively. To detect possible quenching effects of the compounds, CyPet and YPet were detected at ex436/em465 nm and ex500/em535, respectively, at the beginning of each measurement. All fluorescent measurements were performed in a Varioskan microplate reader (Thermo Scientific), in black 96-well plates. For data analysis the linear part of the increase in the fluorescence signal (200−600 s) was fitted by linear regression using Prism software (GraphPad).

In Silico Screening. Using Secin16 as a single template, similarity searching of our in-house virtually formatted compound collection[18] was carried out using the MACCS fingerprint.[33] Compounds were ranked relative to Secin16 in the order of decreasing calculated Tanimoto similarity.[34]

Proliferation Assay. PC9 cells (kind gift of K.Nishio) were grown at 37 °C and 5% CO_2 in RPMI (PAA)/10% FBS (Lonza). For proliferation assay, 3×10^3 PC9 cells per 96 wells were seeded into a clear, flat-bottom 96-well plate (TPP). After 24 h the cells were treated with the respective concentration of compounds or solvent (final DMSO concentration 0.4%) in RPMI, 1% FCS. Medium was changed daily for 3 days, and cell proliferation was analyzed with a 3-(4, 5-dimethylthiazol-2-yl)-2,5-diphenyltetrazolium bromide (MTT) assay as described in the manufacturer's protocol using a Varioscan microplate reader (Thermo Scientific). All assays were performed at least in triplicate. For calculation of the relative proliferation rate/cell number, the mean absorbance in the solvent (DMSO)-only treated cells was set as 1.

■ ASSOCIATED CONTENT

Ⓢ Supporting Information. Additional fluorescence data and complete refs 4 and 30. This material is available free of charge via the Internet at http://pubs.acs.org.

■ AUTHOR INFORMATION

Corresponding Author
m.famulok@uni-bonn.de

■ REFERENCES

(1) D'Souza-Schorey, C.; Chavrier, P. *Nat. Rev. Mol. Cell. Biol.* **2006**, *7*, 347–358.

(2) Bos, J. L.; Rehmann, H.; Wittinghofer, A. *Cell* **2007**, *129*, 865–877.

(3) Kolanus, W. *Immunol. Rev.* **2007**, *218*, 102–113.

(4) Bill, A.; *Cell* **2010**, *143*, 201–211.

(5) Lim, J.; Zhou, M.; Veenstra, T. D.; Morrison, D. K. *Genes Dev.* **2010**, *24*, 1496–1506.

(6) Hafner, M.; Schmitz, A.; Grune, I.; Srivatsan, S. G.; Paul, B.; Kolanus, W.; Quast, T.; Kremmer, E.; Bauer, I.; Famulok, M. *Nature* **2006**, *444*, 941–944.

(7) Fuss, B.; Becker, T.; Zinke, I.; Hoch, M. *Nature* **2006**, *444*, 945–948.

(8) Kahn, R. A.; Randazzo, P.; Serafini, T.; Weiss, O.; Rulka, C.; Clark, J.; Amherdt, M.; Roller, P.; Orci, L.; Rothman, J. E. *J. Biol. Chem.* **1992**, *267*, 13039–13046.

(9) Franco, M.; Chardin, P.; Chabre, M.; Paris, S. *J. Biol. Chem.* **1995**, *270*, 1337–1341.

(10) John, J.; Sohmen, R.; Feuerstein, J.; Linke, R.; Wittinghofer, A.; Goody, R. S. *Biochemistry* **1990**, *29*, 6058–6065.

(11) Lenzen, C.; Cool, R. H.; Wittinghofer, A. *Methods Enzymol.* **1995**, *255*, 95–109.

(12) Kahn, R. A.; Gilman, A. G. *J. Biol. Chem.* **1986**, *261*, 7906–7911.

(13) Nie, Z.; Hirsch, D. S.; Randazzo, P. A. *Curr. Opin. Cell Biol.* **2003**, *15*, 396–404.

(14) Bonifacino, J. S. *Nat. Rev. Mol. Cell. Biol.* **2004**, *5*, 23–32.

(15) Takatsu, H.; Yoshino, K.; Toda, K.; Nakayama, K. *Biochem. J.* **2002**, *365*, 369–378.

(16) Hall, B.; McLean, M. A.; Davis, K.; Casanova, J. E.; Sligar, S. G.; Schwartz, M. A. *Anal. Biochem.* **2008**, *374*, 243–249.

(17) Nguyen, A. W.; Daugherty, P. S. *Nat. Biotechnol.* **2005**, *23*, 355–360.

(18) Stumpfe, D.; Bill, A.; Novak, N.; Loch, G.; Blockus, H.; Geppert, H.; Becker, T.; Schmitz, A.; Hoch, M.; Kolanus, W.; Famulok, M.; Bajorath, J. *ACS Chem. Biol.* **2010**, *5*, 839–849.

(19) Zhang, J. H.; Chung, T. D.; Oldenburg, K. R. *J. Biomol. Screen.* **1999**, *4*, 67–73.

(20) Boulay, P. L.; Cotton, M.; Melancon, P.; Claing, A. *J. Biol. Chem.* **2008**, *283*, 36425–36434.

(21) Li, M.; Wang, J.; Ng, S. S.; Chan, C. Y.; He, M. L.; Yu, F.; Lai, L.; Shi, C.; Chen, Y.; Yew, D. T.; Kung, H. F.; Lin, M. C. *Cancer* **2009**, *115*, 4959–4972.

(22) Muralidharan-Chari, V.; Hoover, H.; Clancy, J.; Schweitzer, J.; Suckow, M. A.; Schroeder, V.; Castellino, F. J.; Schorey, J. S.; D'Souza-Schorey, C. *Cancer Res.* **2009**, *69*, 2201–2209.

(23) Vigil, D.; Cherfils, J.; Rossman, K. L.; Der, C. J. *Nat. Rev. Cancer* **2010**, *10*, 842–857.

(24) Mossessova, E.; Corpina, R. A.; Goldberg, J. *Mol. Cell* **2003**, *12*, 1403–1411.

(25) Viaud, J.; Zeghouf, M.; Barelli, H.; Zeeh, J. C.; Padilla, A.; Guibert, B.; Chardin, P.; Royer, C. A.; Cherfils, J.; Chavanieu, A. *Proc. Natl. Acad. Sci. U.S.A.* **2007**, *104*, 10370–10375.

(26) Bi, X.; Schmitz, A.; Hayallah, A. M.; Song, J. N.; Famulok, M. *Angew. Chem., Int. Ed.* **2008**, *47*, 9565–9568.

(27) Hafner, M.; Vianini, E.; Albertoni, B.; Marchetti, L.; Grüne, I.; Gloeckner, C.; Famulok, M. *Nat. Protoc.* **2008**, *3*, 579–587.

(28) El Azreq, M. A.; Garceau, V.; Harbour, D.; Pivot-Pajot, C.; Bourgoin, S. G. *J. Immunol.* **2010**, *184*, 637–649.

(29) Ikenouchi, J.; Umeda, M. *Proc. Natl. Acad. Sci. U.S.A.* **2010**, *107*, 748–753.

(30) Jones, C. *Nat. Cell Biol.* **2009**, *11*, 1325–1331.

(31) Oh, S. J.; Santy, L. C. *J. Biol. Chem.* **2010**, *285*, 14610–14616.

(32) Torii, T.; Miyamoto, Y.; Sanbe, A.; Nishimura, K.; Yamauchi, J.; Tanoue, A. *J. Biol. Chem.* **2010**, *285*, 24270–24281.

(33) MACCS structural keys; Symyx Software, San Ramon, CA, USA.

(34) Willett, P. *J. Med. Chem.* **2005**, *48*, 4183–4199.